

SYNTHESIS AND CHARACTERIZATION OF Sn₂S₃ AS NANOPARTICLES, POWDERS AND THIN FILMS, USING SOFT CHEMISTRY REACTIONS

R. GODOY-ROSAS^{a*}, S. BARRAZA-FÉLIX^a, R. RAMÍREZ-BON^b,
R. OCHOA-LANDIN^c, H. A. PINEDA-LEÓN^d, M. FLORES-ACOSTA^a,
S. G. RUVALCABA-MANZO^a, M. C. ACOSTA-ENRIQUEZ^a, S.J. CASTILLO^a.

^aPhysics Research Department, University of Sonora, Hermosillo, Son, 83000, Mexico.

^bCINVESTAV, Querétaro Unit, Querétaro, Qro, 76001 Mexico.

^cPhysics Department, University of Sonora, Hermosillo, Son, 83000, Mexico.

^dEngineering and Technology Institute, Autonomous University of Ciudad Juárez, Ciudad Juárez, Chih. 32310 Mexico.

In this paper is proposed a new formulation to obtain Sn₂S₃ nanoparticles, powders, and thin films from aqueous solutions; where the main precursor compounds are a tin salt and a sulfur source. In the intermediate process was used a combination of two complexing agents in order to control the reaction and obtain nanoscale particles, these agents were polyethyleneimine, acetylacetone and a mix of ammonium hydroxide with ammonium chloride. The identification and measurement of the nanoparticles was by DLS, HRTEM, UV-vis, XPS, XRD and Raman Spectroscopy; where direct and indirect bandgaps were 1.65 and 1.31 eV, respectively, the corresponding crystallographic phase was orthorhombic, matching with the Powder Diffraction File, PDF # 14-0619. The calculated sizes were 6 nm by XRD and 13 nm by DLS.

(Received June 4, 2017; Accepted September 2, 2017)

Keywords: Nanoparticles, Tin Sulfide, Materials Characterization, Semiconductors

1. Introduction

In recent times of physics-chemistry, nanotechnology and nanomaterials, the Tin Sulfide is a well-known semiconductor and appears constantly synthesized by soft chemistry [1]. The sulfur ions incorporate metallic and non-metallic elements in complex structures because they are excellent in ionic intercalation [1-3]. Sn and S are abundant in nature, inexpensive and less toxic [1,3-5] than their cadmium and indium competitors used in solar cells [4-8] and optoelectronics [6, 9-10].

In the production of hybrid thin films of SnS₄ and CuInSe₂ the compounds can be replaced by Cu₂ZnSnS₄ to obtain a material with solar conversion parameters like those established [4-5,7-8,11]. Also, to produce energy storage devices, taking advantage of quantum confinement properties of chalcogenides of tin sulfide, it is nowadays a significant target of the photovoltaic industry [1,3-5]. In the green processes for cleaning residual water, the tin is trapped through the aggregation of sulfuric materials whose action synthesizes SnS nanoparticles [2]. The Sn_xS_y compounds crystallize in different phases with at least three basic forms that are classified in terms of their stacking sequence, the most common SnS₂ hexagonal and orthorhombic Sn₂S₃ deposited in thin films as semiconductor and window material, into 2013, tin sulfide nanoparticles were grown in order to form thin films using pressure inert gas [10-14].

In the last three decades, new synthesis of nanoparticles and nanocrystals for binary and hybrid chalcogenide materials have emerged, such as those that have used “sweet” chemistry and SILAR to deposit thin films of tin sulfide and other semiconductors [1]. In 1997 SnS was

*Corresponding author: rodolfogodoyrosas@hotmail.com

deposited for the first time in Sn/S/O layers by evaporation for solar cells, in thin films as a Cadmium free buffer, at temperatures between 300 and 600 °C obtaining a bandgap of 1.1 to 1.5 eV with high optical absorption and intrinsic conductivity type p [3, 14-15]. In 2015, plasma-enhanced chemical vapor deposition (PECVD), Heterojunctions based on SnS and SnS₂ compounds have been prepared [16]. In 2007, thin films of SnS₂ were prepared by growing by using pyrolytic spray technique with SnCl₂ and N, N-dimethyl thiourea precursors and as solvents alcohol, water and hydrochloric acid [1, 11, 17]. In 2014, a route was reported to prepare tin sulfide nanoparticles by direct dispersion of molten tin in solution with sulfur, the process shows blue-ultraviolet emission [3, 13], during the same year, microelectronic applications of monocrystalline SnS nanowires synthesized and deposited by thermal evaporation at hydrogen-argon atmosphere using a quartz tube furnace on gold-coated silicon substrates are reported [9]. More recently in 2015 were deposited SnS thin films with orthorhombic phase using the SILAR technique, from tin chloride and ammonium sulfide, crystal size 45 nm and bandgap 1.63 eV [18]. Finally, in 2016, thin films of nano spheres were deposited by thermal evaporation in the hexagonal phase for SnS₂ and in orthorhombic phase for SnS and Sn₂S₃ [19]. Also, have been published synthesis and applications of compounds SnS, SnS₂ and SnO₂ for uses at lithium-ion batteries, with high storage capacity and good performance as energy supercapacitors [3]. Therefore, we decided to orient our research of nanoparticles of tin sulfide as a final product, see also [2, 9, 16, 18, 20]. We obtained new formulation and synthesis in aqueous solution using soft chemistry reactions, under atmospheric-pressure conditions at 25 °C, with low cost reagents and easy residual management. The technique is based on the addition of the metallic ion from tin dichloride and nonmetallic ion from thioacetamide. For nanoparticles synthesis is used polyethyleneimine as complexing agent and acetylacetone as dispersant in a test tube with deionized water, assisted with electromechanical sonication. In addition, for powders and thin films was used ammonium hydroxide mixed ammonium chloride.

2. Experimental

A first observation that it is necessary to comment is the low solubility of the tin chloride, then due this, we decide to use low molarities for the Tin source. The chemical recipe to grow the Sn₂S₃ nanoparticles, consist to add 1 ml of SnCl₂·2H₂O (0.1 M), 2 ml of Polyethyleneimine (3.5 ml PEI:50 ml H₂O), stirring with an ultrasonic bath for 1 minute; 0.05 ml of concentrate Acetylacetone; after this 0.1 ml of concentrated Acetylacetone is added; then is added 1 ml of Thioacetamide (0.1 M) as sulfur source, stirring again ultrasonically 1 more minute; finally, 4 ml of deionized water were added and was stirred ultrasonically stirred 2 more minutes.

The developed recipe to grow powders and non-homogeneous films consist into aggregate 1 ml of SnCl₂·2H₂O (0.1 M) with 1 ml of Polyethyleneimine (3.5 ml PEI: 50 ml H₂O), plus 0.05 ml of concentrate Acetylacetone; after that it is added 0.15 ml of Buffer [NH₄OH/NH₄Cl] pH 11; then 1 ml of Thioacetamide (0.1 M); finally, 4 ml of deionized water were added and mechanically stirred to posteriorly immerse a glass slide substrate.

Some of the used equipment were: TEM-HRTEM, Jeol-Jem 2010F. UV-vis, Cary WIN 60. XPS PHI-5100. XRD: Bruker Dg. Advance. Raman Spectroscopy, Horiba Javan-Yvan. DLS: Dynamic light scattering detector, Horiba scientific, PD2000 plus.

3. Results

We will start by explaining the HRTEM characterization, this characterization was carried out upon three nanometric regions. In Figure 1, the part a) shown a region of the sample where the global FFT (Fast Fourier Transform was not clear), then we reduced our analysis the analysis area to the selected by a white squared. This lead to the part b), applying a FTT image, from here after a masking process, and the application of inverse FFT, was realized the image c) where interplanar distances were located to identify the chemical compound synthetized using databases.

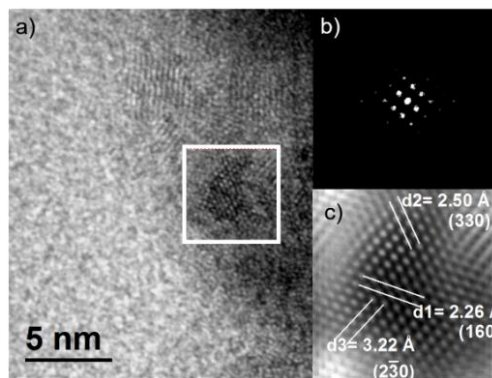


Fig. 1. HRTEM of Sn_2S_3 nanoparticles, a) contrast micrograph and selected analysis area, b) Laue pattern obtained by software and c) inverse FFT

In Fig. 2 is showed a denser amount of particles a), where its complete FFT lead to a bigger Laue pattern b) afterwards, was obtained the part c) where is depicted a better crystallinity view.

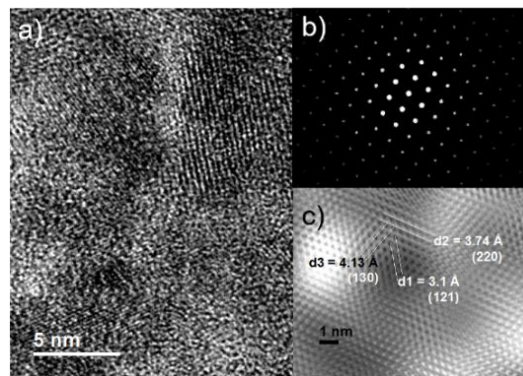


Fig. 2. HRTEM of Sn_2S_3 nanoparticles in part a) is located a denser number of particles as contrast micrograph, in part b) is shown Laue pattern obtained by Software, and in part c) is the corresponding inverse FFT

In Fig. 3 working with higher magnification, the analysis was focused on a single nanoparticle, part a), leading to a more symmetrical Laue pattern, part b), and a better image of inverse FFT, part c).

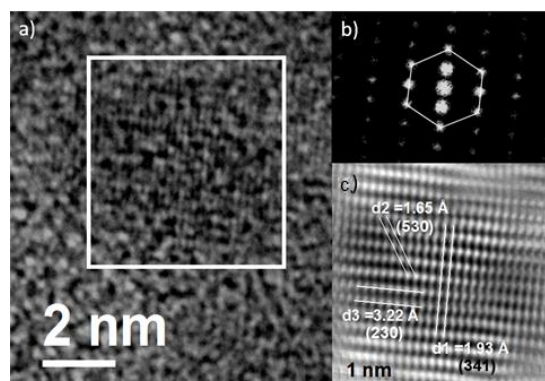


Fig. 3. HRTEM of Sn_2S_3 nanoparticles focused in a single particle, part a) is the contrast micrograph, part b) corresponds to the software obtained Laue pattern, and part c) is the inverse FFT, after a masking process

For all the three regions, the concordance was with the Powder Diffraction File: PDF # 14-0619, of Sn₂S₃ orthorhombic.

The next characterization is the optical absorption in the visible range from 400 to 800 nm wavelength, see Figure 4, from here were evaluated the energy bandgap by the Tauc method obtaining the values of 1.65 eV for the direct band gap and 1.31 eV for indirect band gap, the main curve in Fig. 4 corresponds to the optical absorption of the tin sulfide nanoparticles considered. The insets are depicted the graphical calculations used, by Tauc method as for direct bandgap as indirect bandgap.

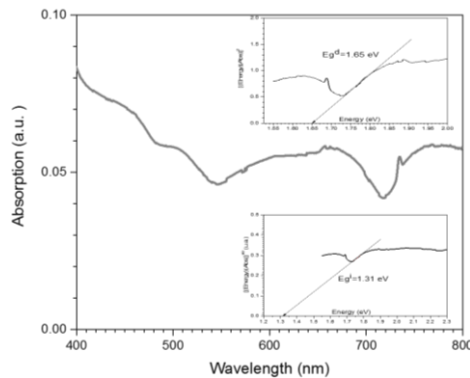


Fig. 4. Optical response by visible spectroscopy for tin sulfide nanoparticles, the up inset corresponds to direct bandgap geometrical calculation, the down inset corresponds indirect bandgap

From the tin sulfide formulation for films were obtained powders, which were used to investigate the crystalline structure of tin sulfide, by X-ray, see Fig. 5, XRD with a wavelength incident ray 1.54 Å, the more accurate coincidence was with the pattern PDF#14-0619 in orthorhombic phase and stoichiometry Sn₂S₃.

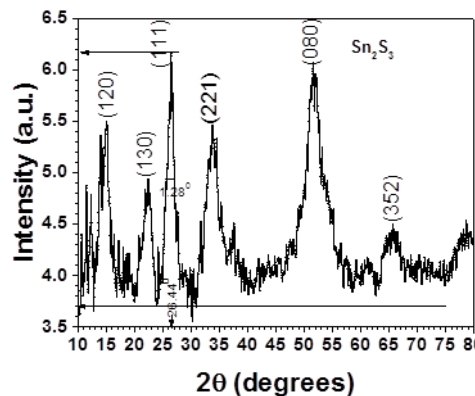


Fig. 5. XRD pattern of tin sulfide, Sn₂S₃, orthorhombic phase

The crystallite size is determined from the XRD pattern, figure 5, by the Debye-Scherrer equation

Where, $\lambda = 1.54 \text{ \AA}$, $B = 1.28^0 \approx 2.234 \times 10^{-2} \text{ rad}$, $2\theta = 26.44^0 \Rightarrow D \approx 6.37 \text{ nm}$

Then the crystallite size is around 6 nm, while that calculating by Dynamical Light Scattering the estimated diameter was around 13 nm.

The XPS measurements were realized on tin sulfide drop coating samples, the used substrate was coring glass slides from which were obtained some signals of elements such as silicon and intensified oxygen, the figure 6 shows a survey spectrum where can be observed Sn, S, O and C, among others. For further comparison, see references [20-21].

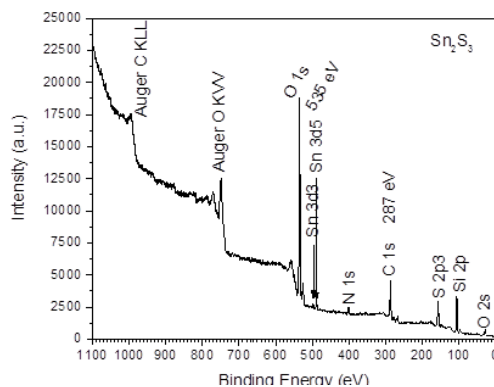


Fig. 6. XPS survey spectrum of drop coating nanoparticles upon a glass slide substrate, shows the elements involved in the nanoparticles of Sn_2S_3

Processing the signals for tin and sulfur was built the Fig. 7 where can be observed the next binding energies Sn $3d_{3/2}$ (497 eV), Sn $3d_{5/2}$ (489 eV), S 2p (157 eV).

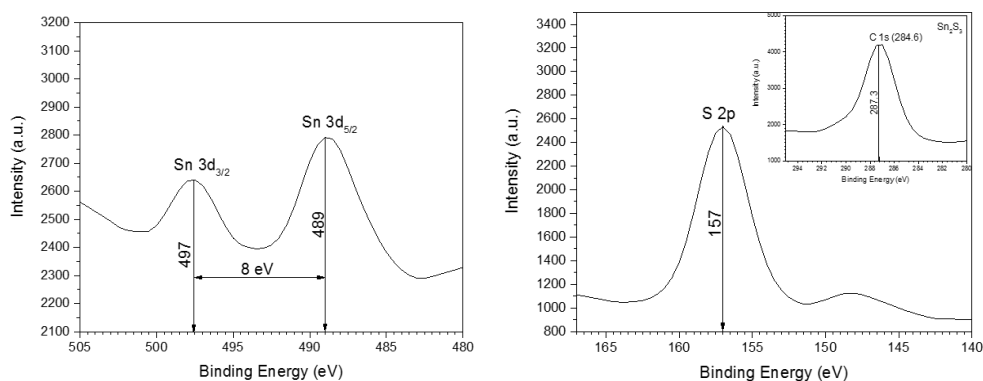


Fig. 7. Amplification and smoothing of the signals for Tin, Sulfur and Carbon, as indicated on the plots

The figure 8 shows the Raman scattering in a shorted range from 80 to 400 cm^{-1} , ten wavenumbers are in the plot of figure 8, for comparison see references [20-21].

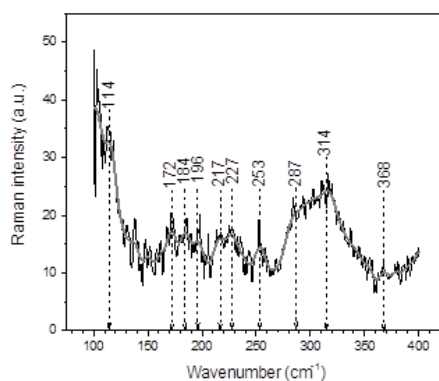


Fig. 8. In that figure can be observed several wavenumbers related with the synthesized compound Sn-S

In Fig. 9, are shown three plots corresponding to transmission (plot 1), Raman scattering (plot 2) and absorption (plot 3). As can be observed the Raman scattering and the absorption are related in certain frequencies bands, these responses are from 400 to 4000 cm^{-1} . Table 1 summarize the experimental values related with transmission, absorption in the infrared range as well as the Raman Scatterings which occur at the same range.

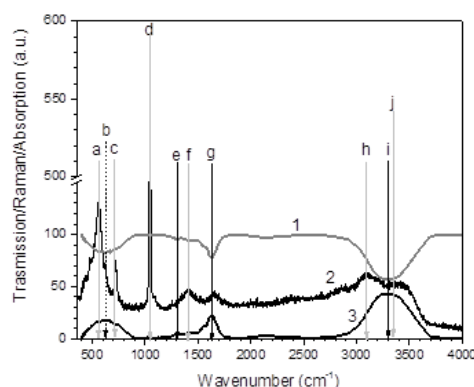


Fig. 9. Correlation between Transmission-Absorption versus the Raman scattering responses

Table 1. Main experimental wavenumbers (frequencies) shown in Fig. 9

Peak	a (R)	b	c(R)	d	e	f(R)	g(R)	h(R)	i	j(R)
Wavenumber (cm^{-1})	565.9	616	723.6	1044.2	1300	1398.7	1634	3112.9	3272	3416.8

4. Discussion

Basically, we synthesize the tin sulfide material, Sn_2S_3 , making to reaction the tin chloride complexed with polyethyleneimine and dispersed it with acetylacetone; with the Thioacetamide, this process give to us nanoparticles, while that if is added a buffer solution of $\text{NH}_4\text{OH}/\text{NH}_4\text{Cl}$ of pH 11, we get adherence on an immersed glass substrate in the reactor, as well as powder precipitate.

Our main characterizations were HRTEM, XRD and optical absorption, offering us the possibility to identify the synthesized Sn_2S_3 as a semiconductor in orthorhombic phase. Other realized characterizations, let us to observe the existent correlation within Transmission-Absorption in the IR range versus the Raman scattering at the same range. From figure 7, of XPS spectra, we observed fundamentally that the Carbon peak is shift until 287.3 eV (which should be 284.6), and the difference between the Sn-3d peaks was not 8 eV instead 8.5 eV. That lead us to purpose the stoichiometric form assumed for the tin sulfide.

5. Conclusions

By contrasting our formulation and method used, with other methods reported and mentioned in the introduction, we observe that ours is very simple. The developed recipe is reproducible, which is an indicative that the nanoparticles obtained are very stable under normal laboratory conditions.

The Nanoparticles have sizes of 6 nm from XRD/Debye-Scherrer and 13 nm from Dynamical Light Scattering calculations.

Acknowledgments

Dra Judith Tanori (HRTEM, Viscosity measurement), MC Abraham Mendoza (XRD), MC Roberto Mora (XPS), Dr. Roberto Carrillo (Raman), Dr Heriberto Acuña (refraction index measurement), Dr Ricardo Esparza (DLS); we want to thank for the facilities to use the equipment for realize the characterizations. Also, the support provides by CONACYT and CINVESTAV Qro-Instituto politécnico Nacional.

References

- [1] T. Jiang, G. A. Ozin, *J. Mater. Chem.*, **8**(5), 1099 (1998).
- [2] J. Gaur, S. Jain, S. Chand, N. K. Kaushik, *American Journal of Analytical Chemistry* **5**, 50 (2014).
- [3] K. Li, S. Yan, Z. Lin, Y. Shi, *Journal of Alloys and Compounds*, **681**, 486 (2016).
- [4] H. Katagiri, K. Jimbo, W. S. Maw, K. Oishi, M. Yamazaki, H. Araki, A. Takeuchi, *Thin Solid Films*, **517**, 2455 (2009).
- [5] K. Muska, M. Kauk, M. Altosaar, M. Pilvet, M. Grossberg, O. Volobujeva, *Energy Procedia*, **10**, 203 (2011).
- [6] C. Calderón, G. Gordillo, E. Banguero, P. Bartolo-Pérez, M. Botero, *Revista Mexicana de Física* **62**, 484 (2016).
- [7] T. J. Whittles, L. A. Burton, J. M. Skelton, A. Walsh, T. D. Veal, V. R. Dhanak, *Chemistry of Materials* **28**, 3718 (2016).
- [8] F. Hergert, R. Hock, *Thin Solid Films* **515**, 5953 (2007).
- [9] S.R. Suryawanshi, S.S. Warule, S.S. Patil, K.R. Patil, M.A. More, *ACS Applied a. Material and Interfaces* **6**, 2018 (2014).
- [10] A. Sanchez-Juarez, A. Ortiz, *Journal of The Electrochemical Society* **147**(10), 3708 (2000).
- [11] K. Jimbo, R. Kimura, T. Kamimura, S. Yamada, W. S. Maw, H. Araki, K. Oishi, H. Katagiri, *Thin Solid Films*, **515**, 5997 (2007).
- [12] V. Robles, J.F. Trigo, C. Guillén, J. Herrero, *Energy Procedia*, **44**, 96 (2014).
- [13] Y. Zhao, Z. Zhang, H. Dang, W. Liu, *Materials Science and Engineering: B*, **113**, 175 (2004).
- [14] O.E. Ogah, G. Zoppi, I. Forbes, R.W. Miles, "23rd European Photovoltaic Solar Energy Conference", Valencia Spain, **1-5** 2008.
- [15] L.S. Price, I.P. Parkin, A.M.E. Hardy, R.J. H. Clark, *Chemistry of Materials*, **11**, 1792 (1999).
- [16] A. Sanchez-Juarez, A.T. Silver, A. Ortiz, *Thin Solid Films*, **480-481**, 452 (2005).
- [17] M.C. Rodríguez, A.S. Juárez, "Superficies y Vacío", **20**(1), 34-38 2007.
- [18] A. Mukherjee, P. Mitra, *Materials Science-Poland*, **33**(4), 847 (2015).
- [19] F. Sheini, M. Cheraghizade, R. Yousefi, *Solar Energy Materials & Solar Cells* **154**, 49 (2016).
- [20] M. M. Bletskan, D. I. Bletskan, *J. Optoelectron. Adv. M.* **16**(5-6), 659 (2014).
- [21] J. Li, J.Huang, Y.Zhang, Y.Wang, C. Xue, G. Jiang, W. Liu, Ch. Zhu, *RSC Advances* **6**, 58786 (2016).
- [22] Keyu Li, Shancheng Yan, Zixia Lin Yi Shi, *Journal of Alloys and Compounds* **681**, 486 (2016).